ATMOSPHERIC SCIENCE LETTERS
Atmos. Sci. Let. **13**: 139–150 (2012)
Published online 27 March 2012 in Wiley Online Library
(wileyonlinelibrary.com) **DOI:** 10.1002/asl.376

RMetS
Royal Meteorological Society

A Joss–Waldvogel disdrometer derived rainfall estimation study by collocated tipping bucket and rapid response rain gauges

Tanvir Islam,* Miguel A. Rico-Ramirez, Dawei Han and Prashant K. Srivastava
Department of Civil Engineering, University of Bristol, Bristol BS8 1TR, UK

**Correspondence to:
T. Islam, Department of Civil Engineering, University of Bristol, Bristol BS8 1TR, UK. E-mail: tanvir.islam@bristol.ac.uk*

Received: 24 July 2011
Revised: 23 December 2011
Accepted: 27 February 2012

Abstract

This article studies the rainfall estimates derived from a Joss–Waldvogel disdrometer, using an extensive dataset of raindrop spectra for the period of 2003–2010. Four rain gauges (one tipping bucket and three rapid response drop counting devices) are employed for the appraisal with the disdrometer observations. The appraisal has been carried out in view of hourly rainfall accumulations, time series accumulative rainfall, and rain rate observations. From the yearly timescale statistics, the correlation between the disdrometer derived hourly rain accumulations to those measured by the rain gauges are in the range of 0.89–0.99 (mean absolute error, 0.10–0.45 mm, and normalized mean bias −1.03% to −50.28%). Especially, the estimated rainfall by the tipping bucket rain gauge is in sound agreement with the disdrometer observations, which is also reflected in time series accumulative rainfall comparisons, showing no more than 20% differences roughly. On the other hand, the results reveal that regardless of any influence of the integration period, the agreement between the disdrometer and the three rapid response rain gauges are quite consistent. Nevertheless, the association of the tipping bucket rain gauge is sensitive to the integration periods. In fact, increasing the integration period improves the rain rates agreement. Further to the appraisal for various rain classes, there is an underestimation to overestimation trend of disdrometer estimated rain rates with the increase of rain classes. Copyright © 2012 Royal Meteorological Society

Keywords: **precipitation uncertainties; small-scale variability; raindrop spectra; drop size distribution; radar errors; instrumental measurements; stratiform and convective**

1. Introduction

Disdrometer is an integral component in radar remote sensing research and operations. It can measure drop size distributions (DSD), the fundamental characteristic in radar-based precipitation estimation. By providing the knowledge of DSDs, the instrument has shown a great potential in radar adjustment, reflectivity monitoring, and identifying key sources of errors in radar rainfall estimation. For instance, Lee and Zawadzki (2006) used a long time record of DSDs and stated that disdrometric radar adjustment was not affected by DSD variability. Miriovsky *et al*. (2004) conducted an experimental study using four disdrometers to look at the small scale spatial variability of radar reflectivity, which contributes to the error in rainfall estimation. Lee (2006) also examined the sources of errors in polariometric radar rainfall estimation using long-term disdrometric data. Moreover, radar rainfall algorithm developments considerably rely on disdrometer observations of DSDs. For many years, numerous studies have been carried out to identify a suitable empirical equation relating the radar reflectivity (Z) to rain rate (R) based on DSDs (Cerro *et al*., 1997; Atlas *et al*., 1999; Campos and Zawadzki, 2000; Rico-Ramirez *et al*., 2007). Recent advancement in radar rainfall estimation using polarimetric radar estimators is also established from disdrometer raindrop spectra observations (Ryzhkov and Zrnic, 1995; Brandes *et al*., 2002; Matrosov *et al*., 2002; Bringi *et al*., 2011). Additionally, radar data quality improvement studies, such as attenuation correction at higher frequency through scattering simulation of disdrometer data are reported. One such attenuation correction studies was carried out by Bringi *et al*. (2006), where they simulated various polarimetric relations from disdrometer DSD by utilising the scattering parameters of specific attenuation and specific differential attenuation against specific differential phase, which were then corrected to the measured reflectivity and differential reflectivity for attenuation. Park *et al*. (2005) also evaluated an attenuation correction methodology for multi-parameter X-band radar with disdrometer simulated data. Another contribution of the instrument in radar remote sensing research is validation of satellite borne precipitation radar data for global rainfall estimation (Houze *et al*., 2004; Kozu *et al*., 2009).

Along with the optical disdrometers, impact type Joss–Waldvogel (JW) disdrometers are being widely used for various radar and atmospheric research since their invention in 1967 (Joss and Waldvogel, 1967; Bringi *et al*., 2003; Wolff *et al*., 2005). However, a number of limitations regarding the JW disdrometer performance are raised. One such limitations is the background atmospheric noise (Tokay *et al.*, 2003). It has also been reported that impact type JW disdrometer often miscounts drops in lower size bins, in particular, for drops of lesser than 1 mm diameter. It also cannot differentiate large drops and places drops greater than 5 mm in its last bin (Tokay *et al.*, 2002). Sometimes, two or more drops reach the surface cross section of the disdrometer simultaneously, resulting in a miscounting of the rain drops. To overcome this problem, an error correction multiplication matrix is currently provided by the manufacturer based on the correction scheme of Sheppard and Joe (1994). Another shortcoming of the disdrometer is that it cannot measure the terminal velocity of falling drop and this velocity usually needs to be assumed. In contrast, an optical disdrometer has the capability of observing the fall velocity of a drop, and is sometimes preferred over the JW disdrometer. Nevertheless, optical disdrometers are also not free from errors and omissions. Moumouni *et al.* (2008) compared three optical disdrometers using tipping bucket rain gauges and found correlation as low as 0.85. In fact, the JW disdrometer is generally accepted to be the standard instrument for drop size distribution measurement as stated in Tokay *et al.* (2005).

The objective of this article is to assess how close the JW disdrometer derived rainfall estimates agree with rain gauge measurements. In the past, a number of studies have been conducted to address the query, e.g. those by Radhakrishna and Rao (2010), Wang *et al.* (2008), Tokay *et al.* (2003), Tokay *et al.* (2002). However, the studies reported in the literature so far are based on short-term datasets (i.e. only a few months), and the number of long-term studies is limited. In this study, we assess rainfall estimates from a JW disdrometer with four rain gauges over a long-term dataset of observations (years 2003–2010). It is expected that this extensive dataset will provide a clear idea of performance between the impact type JW disdrometer and rain gauges in a long-term perspective. Moreover, two different types of rain gauges (tipping bucket and rapid response drop counting) are employed in the study to judge the results in a scrupulous way. There are numerous publications regarding tipping bucket rain gauges; however, hardly any study is focused on rapid response drop counting rain gauges. On top of that, this work can also be considered as a reference for measurement variation of tipping bucket and rapid response rain gauges with respect to the disdrometer.

2. Dataset and methodology

2.1. Disdrometer

The disdrometer dataset has been acquired using a Disdromet Joss Waldvogel Impact Disdrometer RD-69, installed at Chilbolton facility for atmospheric and radio research (51.1445 °N, 1.4370 °W) and run by the Chilbolton group of the space science and technology department at Rutherford Appleton Laboratory. The data were available from April 2003 to March 2010, excluding mid-August 2004 to mid-December 2004 and July 2005 to May 2006 because of instrumental malfunction and nonoperation. The RD-69 disdrometer consists of two units (Distromet, 1997). One of the units is a sensor, which is exposed to rain and the other one is a processor for analogue processing and digitizing of the sensor measured information. The sensor consists of an electromechanical unit, and an amplifier housed in a common case. It works by converting the vertical momentum of a falling drop into signals. The output information is voltage amplitude, which is a measure for the size of the drop that caused it, and it is allied to the drop diameter with the following equation (Joss and Waldvogel, 1977; Sheppard, 1990):

$$V_L = k.D^n \quad (1)$$

where D is the drop diameter, V_L is the output voltage, and k and n are the calibration constants. The value for k is usually 0.02586, and n ranges between 3.1 and 4.3. Afterwards, a pulse height analyser, embedded in the processor unit, classifies the peaks amplitude V_L, and accordingly, the impacting drop diameters into n_i classes.

The drop size distribution (DSD) at the discrete instant t (in seconds) can be calculated by (Montopoli *et al.*, 2008):

$$N_m(D_i, t) = \frac{n_i(t)}{A.dt.v_i.dD_i} \quad (2)$$

where m indicates a measured quantity; D_i is the central drop diameter of the channel c_i in mm; $N_m(D_i, t)$ is the number of raindrops per unit of volume in the channel c_i at the discrete instant t in units per millimetre per cubic meter; $n_i(t)$ is the number of drops counted in the ith channel at the instant t; A is the sensor area in square meters; dt is the time interval in seconds; v_i is the terminal velocities of raindrops in meters per second; dD_i is the ith bin width in millimetres.

The terminal velocity is assumed as a function of the particle diameter by Atlas and Ulbrich (1977):

$$v_i = 3.78D_i^{0.67} \quad (3)$$

Following the computation of $N_m(D_i, t)$, the rain rate R_m is calculated through the moments of order 3.67, as specified by:

$$R_m(t) = 3.78 \times \frac{\pi}{6} \times m_{3.67}(t) \quad (4)$$

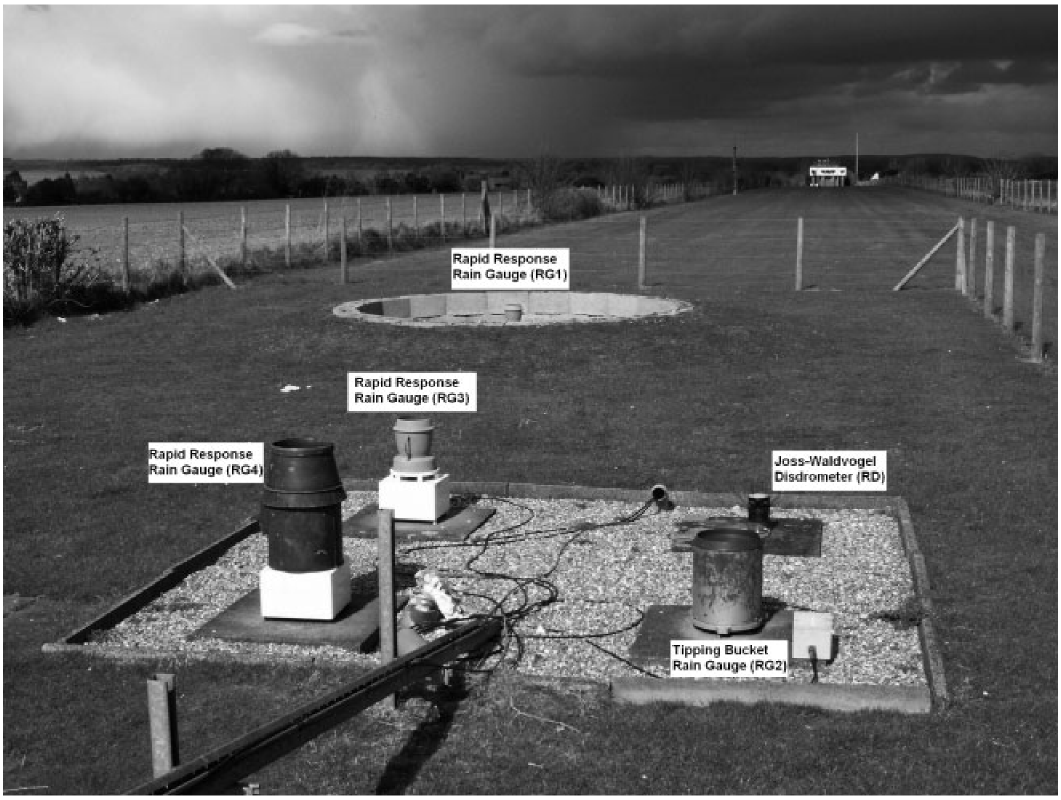

Figure 1. Layout showing the location of the four rain gauges with respect to the disdrometer at the Chilbolton observatory.

where, $m_{3.67}(t)$ is given by:

$$m_{3.67}(t) = \int_0^{\infty} D^{3.67} \times N(D, t) \times dD = \sum_{i=1}^{n_c} D_i^{3.67} \times N_m(D_i, t) \times dD_i \qquad (5)$$

At Chilbolton, drop counts are available every 10 s over 127 bins ranging from 0.3 to 5 mm, and the disdrometer sampling area is given as 50 cm^2. However, as the DSD is a function of time interval, intrinsic noise may occur in the processes. In this study, we have used one minute as the time interval to derive DSD, and ultimately rain rates as the final product. Moreover, we have applied special 'rain partition filter' to separate raindrop spectra from snowfall based on wet bulb temperature (WBT) observations. WBT is known as a good separator of rain and snow. In general, snow is probable only if ground WBT falls below 2 °C and some other atmospheric criteria are satisfied. In this work, we have used WBT = 3 °C as separator and discarded all the values below this threshold.

2.2. Rain gauges

The four rain gauges used in this study were colocated nearby to our disdrometer (RD) at the Chilbolton observatory within a few meters of each other. A layout showing the location of the rain gauges with respect to the disdrometer is illustrated in Figure 1. Two types of rain gauges are used, three RAL rapid response drop counting rain gauges (denoted as RG1, RG3, and RG4 in the figure), and a RW Munro tipping bucket rain gauge (TBR, denoted as RG2 in the figure). More specifically, the RG1 is positioned in a pit within a circular low turf wall enclosure of 3 m diameter on the ground. Other four instruments are in a square base at a distance of approximately 8.5 m from the pit. The sides of the square on which these four instruments (RD, RG2, RG3, and RG4) sit are approximately 1.6 m in length. Generally speaking, special care is taken by the Chilbolton staff to make sure that the data quality of the rain gauges is up to the highest standard.

The TBR rain gauge is the one, which is most common and widely accepted as a standard type for rainfall measurements. It measures rainfall in increments of one tip (0.2 mm). On the other hand, the rapid response drop counting gauges give readings by individual drops rather than giving tip counts with a known constant volume as they pass an optical sensor. That means a single drop is equivalent to a known constant volume of precipitation, compared to the standard tipping bucket gauge, which produces 0.2 mm accumulations per tip. Among the rapid response gauges, RG1 and RG3 use standard size 150 cm^2 collectors having 0.004 mm as a known constant volume of single drop. Whereas, the RG4 uses a larger collector of 324 cm^2, thus providing better resolution at low rain rates with 0.00185 mm accumulation of precipitation. For clarity, the working principle of the rapid response rain gauge is somewhat different from the disdrometer. The rapid response rain gauge counts

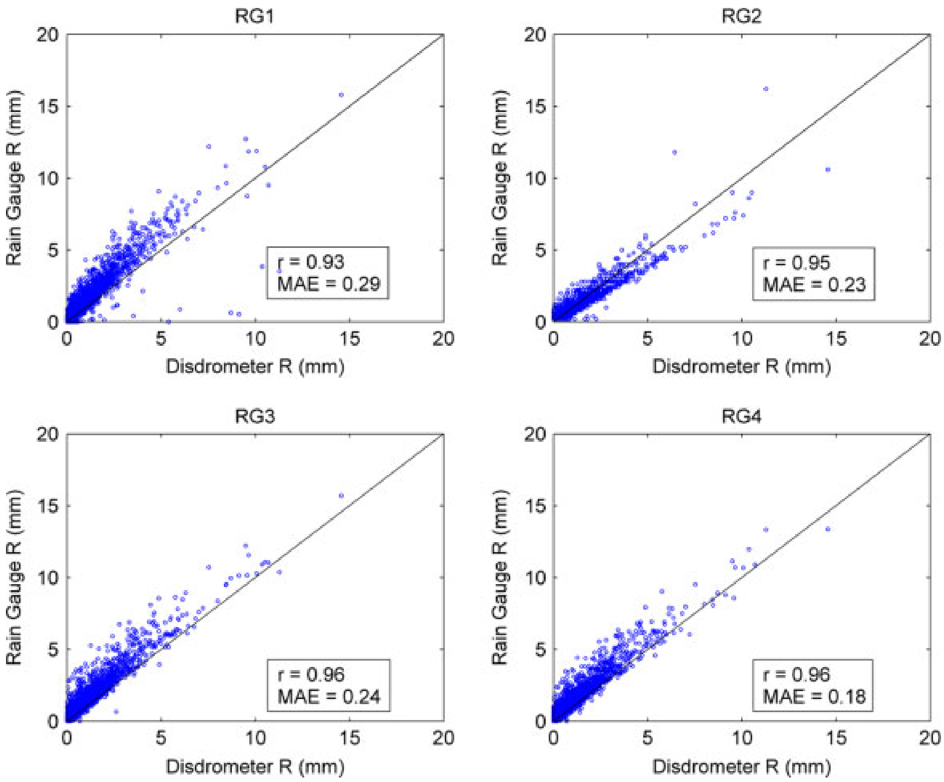

Figure 2. Scatter plots of hourly rain accumulations between disdrometer and four rain gauges (RG1, RG2, RG3, and RG4) for the entire available dataset (2003–2010).

drops of a specific volume, while disdrometer counts actual rain drops instead. Regarding that, the rapid response rain gauge systems are specially designed and developed by the Chilbolton facility, and the design principle can be found in Norbury and White (1971). The readers may also refer to the technical specifications of the Chilbolton rapid response rain gauges in http://www.stfc.ac.uk/Chilbolton/resources/PDF/DropCountingRaingauge.pdf

2.3. Meteorological data

The meteorological data, that is, the wet bulb temperature and the wind speed, have been used in this work for the separation of snowfall conditions and understanding wind speed effects on the assessment (see next section). The datasets are taken from the nearest Met Office – MIDAS Land Surface Observation Station to the instruments, located in Middle Wallop (51.1493 °N, 1.5685 °W).

3. Results and discussion

To check the agreement, the disdrometer derived rainfall estimates are assessed in terms of hourly accumulations, time series accumulative rainfall, and rain rates using four rain gauges as references. Mainly, three statistical parameters are used as performance indicators for the assessment: the coefficient of correlation (r), mean absolute error (MAE), and normalized mean bias (NMB). The coefficient of correlation, mean absolute error, and normalized mean bias are given as follows:

$$r = \frac{\sum_{i=1}^{n}(R_G - \overline{R_G})(R_D - \overline{R_D})}{\sqrt{\sum_{i=1}^{n}(R_G - \overline{R_G})^2}\sqrt{\sum_{i=1}^{n}(R_D - \overline{R_D})^2}} \quad (6)$$

$$MAE = \frac{1}{n}\sum_{i=1}^{n}|R_D - R_G| \quad (7)$$

$$NMB = \frac{\frac{1}{n}\sum_{i=1}^{n}(R_D - R_G)}{\frac{1}{n}\sum_{i=1}^{n}R_G} \quad (8)$$

where n is the number of samples, R_G and R_D represent rain gauge and disdrometer measurements, respectively. In this work, the MAE is given in mm and the NMB is given in percentage unless otherwise stated.

3.1. Hourly rain accumulations

Figure 2 shows the scattergram of hourly rain accumulations obtained from the disdrometer compared to the four different rain gauges (RG1, RG2, RG3, and RG4) for the period of 2003–2010. This figure is accompanied by Table I, in which, yearly statistical relations are given as well. The statistics indicate that the

Table I. Statistical performance of the JW disdrometer-derived hourly rain accumulations with respect to the four rain gauges (RG1, RG2, RG3, and RG4). Study period is 2003–2010.

	RG1			RG2			RG3			RG4		
Year	Coefficient of correlation, r	Mean absolute error, *MAE* (mm)	Normalized mean bias (%)	Coefficient of correlation, r	Mean absolute error, *MAE* (mm)	Normalized Mean Bias (%)	Coefficient of correlation, r	Mean absolute error, *MAE* (mm)	Normalized mean bias (%)	Coefficient of correlation, r	Mean absolute error, *MAE* (mm)	Normalized mean bias (%)
2003	0.95	0.24	−29.18	0.89	0.28	−18.65	0.92	0.45	−50.28	0.93	0.33	−45.20
2004	0.95	0.30	−29.87	0.93	0.22	−3.46	0.94	0.27	−30.60	0.95	0.22	−30.61
2005	0.98	0.25	−38.70	0.97	0.16	−1.13	0.97	0.18	−24.44	0.98	0.13	−24.75
2006	0.93	0.26	−18.31	0.99	0.29	19.57	0.99	0.15	−11.26	0.99	0.10	−6.54
2007	0.89	0.28	−26.00	0.94	0.26	19.92	0.98	0.15	−13.49	0.99	0.11	−9.73
2008	0.97	0.32	−34.03	0.97	0.21	10.54	0.97	0.22	−23.32	0.97	0.17	−19.11
2009	0.97	0.35	−43.22	0.97	0.18	−12.95	0.97	0.30	−36.19	0.97	0.24	−32.99
2010	0.98	0.27	−40.07	0.96	0.13	−10.20	0.98	0.25	−35.32	0.98	0.21	−32.71
All	0.93	0.29	−32.65	0.95	0.23	3.02	0.96	0.24	−27.23	0.96	0.18	−23.89

disdrometer derived hourly rain accumulations agree quite well with those measured by the rain gauges. According to yearly statistics, the Pearson coefficients of correlation are identified in the range of 0.89–0.99, and mean absolute errors are noted between 0.10 and 0.45 mm. The correlations obtained herein are quite consistent throughout the study period, and very similar to those obtained by Radhakrishna and Rao (2010) in cyclonic storm cases. Particularly, the data points between the RG2 and RD are close to the 'true line', reflecting very good agreement between the instruments with $r = 0.95$, $MAE = 0.23$ mm, and NMB $= 3.02\%$. On the other hand, the respective correlations for RG1, RG3, and RG4 are found as 0.93 (MAE = 0.29 mm, NMB = −32.65%), 0.96 (MAE = 0.24 mm, NMB = −27.23%), and 0.96 (MAE = 0.18 mm, NMB = −23.89%). Although, the resulting correlations for the rapid response gauges (RG1, RG3, and RG4) are comparable to the TBR, they give systematically higher hourly accumulations than the disdrometer, as the figure shows. It is to be regarded that the rainfall accumulations from the rapid response gauges contain the samples having low rain intensities. However, according to the design of the rapid response gauges, data during low rain intensities (e.g. less than 1 mm h^{-1}) cannot be reliably used. Therefore, some of the errors may have encompassed in the hourly accumulations, resulting in overestimation. Moreover, although the rapid response gauges collocate to the disdrometer within a few meters, additional discrepancies could be due to random instrumental errors (Ciach, 2003). Indeed, the inter-comparison scatter plots between the rapid response rain gauges illustrated in Figure 3 confirm the random errors and small scale spatial variability, especially when associating RG1 with RG3 and RG4, which is relatively far placed in the pit. Such errors may originate from several sources, for instance, discrete time effect on samples collection, effects of turbulent airflow surrounding the gauges.

3.2. Time series accumulative rainfall

Time series of accumulative rainfall plots from the disdrometer and four rain gauges for the year of 2003–2010 are presented in Figure 4. To maintain the time series, the missing and discarded (applying raindrop filter) data are allocated as non-rainy cells (zero value), and shown as missing values (MV) in the abscissa. Numerical accumulations with differences between rain gauges and disdrometer are given in Table II. Taking disdrometer derived rainfall as reference, positive difference indicates overestimation of the rain gauge values, while negative difference represents underestimation. Note that during the MV period, all the data points from all five instruments have been removed. If we consider the best rain gauge accumulation analogous (least difference) to the disdrometer accumulations for each individual year (shown bold in the Table II), we can conclude that the disdrometer and best corresponding gauge rain totals are in

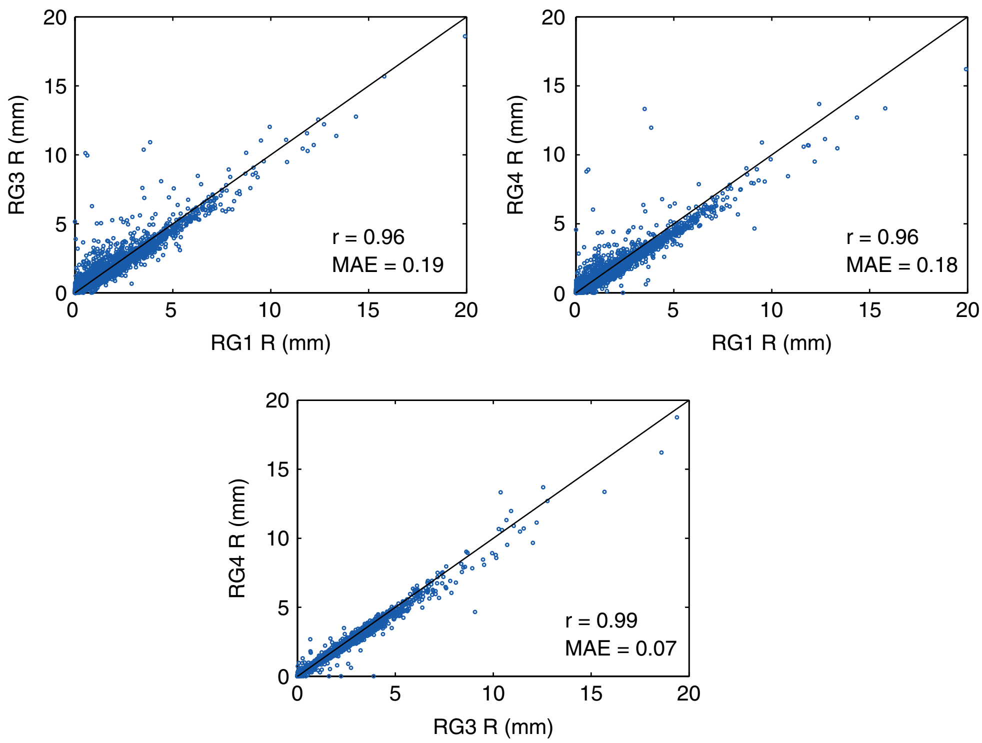

Figure 3. Inter-comparison scatter plots between the rapid response drop counting rain gauges for the entire available dataset (2003–2010).

excellent agreement. The 'best in agreement' rain differences over yearly timescales are found in the range of 1.12% (year 2003) to −13.97% (year 2008). Several researchers have shown that event rain total variation between disdrometer and rain gauge lies within 10–20% (Hagen and Yuter, 2003; Tokay *et al.*, 2003). Manufacturer also claims that rainfall event measurement by JW disdrometer over 5–10 mm accumulation, should not fluctuate by more than 15% as those measured from rain gauges (Tokay *et al.*, 2005). In our case, the rain accumulations are calculated for the entire available yearly dataset, and the 'best in agreement' rain totals are within 15% difference. However, we cannot strongly comment which of the rain gauges demonstrates better agreement in terms of cumulative rainfall. The bias between different rain gauges respective to the disdrometer is not systematic, but variable between years. In 2006 and 2007, the RG4 has displayed better match, while RG2 has shown good agreement in other years. In view of the entire available data (2003–2010), the RG2 has shown very good agreement measuring 2981.60 mm rain accumulations as opposed to the disdrometer accumulations of 3348.87 mm with only 10.97% difference. Moreover, the performance of the tipping bucket rain gauge RG2 throughout all the years is also stable showing differences of 1.12 to −21.01% only, which are within the range of error studies for tipping bucket rain gauge as those found by other authors (Tokay *et al.*, 2002; Wang *et al.*, 2008). In contrast, relatively, inconsistencies are found in rapid response rain gauges. From the statistics, it is apparent that rapid response gauges have generally overestimated the rain totals, whereas a small underestimation is shown for the tipping bucket rain gauge. It can be seen that such overestimation by the rapid response gauges can be as high as over 100%, as for RG3 in 2003. In fact, the differences in some years are considerably large. This might be due to the fact that the rapid response gauge assumes a constant drop size while in the real case, the raindrop sizes are widely variable. As shown in Figure 3, local random errors may also have contributed disparities to the results. It is also to be remembered that the datasets from the rapid response gauges consist of samples with low rain intensities, which would have resulted in further errors.

3.3. Rain rates

The investigation now focuses on rain rate estimation by the JW disdrometer in comparison with the rain gauges. The investigations are carried out considering different integration periods, against wind speed, and for stratiform and convective rain clusters.

a. Different integration periods

As sampling integration period influences the rain rate estimates by the sensors, the comparisons are conducted for five different integration periods (1, 5, 15, 30, 60, 120 min). Figure 5 presents the disdrometer intended statistical measures r, MAE and NMB against four rain gauges as a function of integration periods. As highlighted by the figure, there is a little impact on sampling integration period for disdrometer derived rain rate estimates when comparing with the rapid response gauges RG1, RG3, and RG4. There is a good

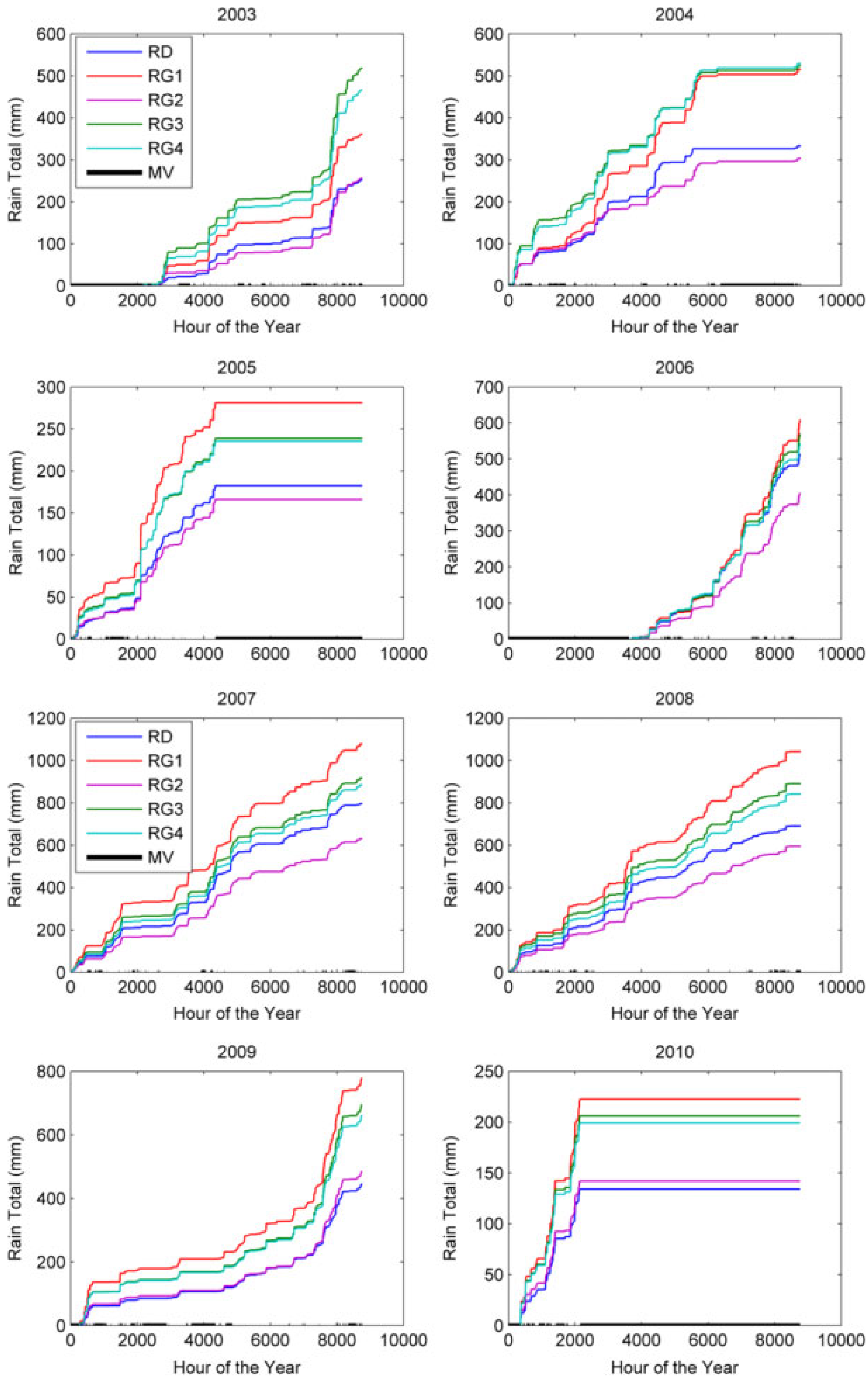

Figure 4. Time series diagram of accumulative rainfall from JW disdrometer and four rain gauges for the period of 2003–2010. The black lines on the abscissa denote missing and discarded cells.

agreement between disdrometer and rain gauges. Especially, RG3 and RG4 show good agreement to the RD with correlation above 0.9, MAE below 1 mm h^{-1}, and NMB within -30%. However, as expected, TBR is sensitive to the integration period and has a poor performance at short integration periods. Previously, numerous authors have confirmed that increasing integration period evidently improves the results of TBR estimates (Habib *et al*., 2001). In our case, the agreement between the RD and RG2 becomes close and comparable to the RG1, RG3, and RG4 when using the integration period of 5 min or more, which is

Table II. Accumulative rainfall from disdrometer (RD) and four rain gauges (RG1, RG2, RG3, and RG4) for the year of 2003–2010[a].

Year	RD	RG1		RG2		RG3		RG4	
	Accumulations (mm)	Accumulations (mm)	Difference	Accumulations (mm)	Difference	Accumulations (mm)	Difference	Accumulations (mm)	Difference
2003	252.57	360.91	42.90%	**255.40**	**1.12%**	518.54	105.31%	466.84	84.84%
2004	333.25	515.55	54.70%	**303.20**	**−9.02%**	523.90	57.21%	529.64	58.93%
2005	182.54	281.08	53.98%	**166.20**	**−8.95%**	238.78	30.81%	235.32	28.91%
2006	513.74	609.44	18.63%	405.80	−21.01%	569.48	10.85%	**543.24**	**5.74%**
2007	796.79	1077.90	35.28%	630.60	−20.86%	916.31	15.00%	**884.48**	**11.00%**
2008	690.71	1042.19	50.89%	**594.20**	**−13.97%**	891.14	29.02%	841.61	21.85%
2009	445.31	777.59	74.62%	**484.00**	**8.69%**	694.21	55.89%	660.12	48.24%
2010	134.05	222.67	66.12%	**142.20**	**6.08%**	206.06	53.73%	199.10	48.53%
All	3348.87	4887.32	45.94%	**2981.60**	**−10.97%**	4558.41	36.12%	4360.34	30.20%

[a] The differences between the disdrometer and the rain gauges are also shown, where positive and negative difference indicates overestimation and underestimation of the rain gauge values corresponding to the disdrometer respectively. The best rain gauge correspondence (least difference) to the disdrometer is shown in bold format.

similar to those found by Frasson *et al.* (2011). Interestingly, by further increasing the integration period (e.g. integration periods larger than around 20 min), the RG2 gauge outperforms the rapid response gauges when comparing to the RD. For instance, at or above 10 min integration period, the revealed NMB is close to 0%.

Considering that the comparison between the disdrometer and the rain gauges are exaggerated to rain intensities as well as integration period, therefore the calculated NMB are presented in Figure 6 as contour plots as a function of integration period and rain classes. Note that the rain classes considered herein represent a wide range of rain intensities (see Table III, from class 1 to class 8) which are created in such a manner so that each class contains sufficient samples for analysis. Remarkably, the contour plots reveal an underestimation to overestimation trend of disdrometer estimated rain rates with the increase of rain classes. This is true when comparing with the all four rain gauges (RG1 to RG4). Similarly, from the discussion for Figure 5, no noticeable consequence of the integration period is observed for the rapid response gauges; but, TBR significantly overestimates the rain intensities at short integration periods, below 10 min for example.

b. Wind speed effects

Some of the past studies exhibit that windy conditions have influence on the measurement accurateness of the disdrometer (Yuter *et al.*, 2006). Especially in strong wind conditions, the performance of rain rate estimation can be degraded. With the intention of investigating this, the rain rate differences between our disdrometer and any of the four rain gauges are shown as a function of wind speed in Figure 7. Note that the sampling integration period is considered as 15 min. By examining the negative correlation coefficients, it is evident that there is no significant association of wind speed on the rain rate deviations between the disdrometer and the gauges. The results revealed here can be related to a recent study of Jaffrain and Berne (2011), where no effect of wind speed was found in their experiment. It must also to be accounted that the rain gauge measurements may also contribute the wind induced systematic error in the rain rate estimation. Generally, the wind induced error for rain gauge measurement is an average of up to 10% (Sieck *et al.*, 2007). Nonetheless, the wind induced errors for those rain gauges placed on ground can be considered somewhat minimal.

c. Stratiform and convective rain clusters

The rain rate estimation performance between the sensors in stratiform and convective rain is of particular interest. To facilitate this, the disdrometer derived raindrop spectra are subdivided into stratiform and convective rain clusters as per the approach of Bringi *et al.* (2003), and Marzano *et al.* (2010). To summarize, if

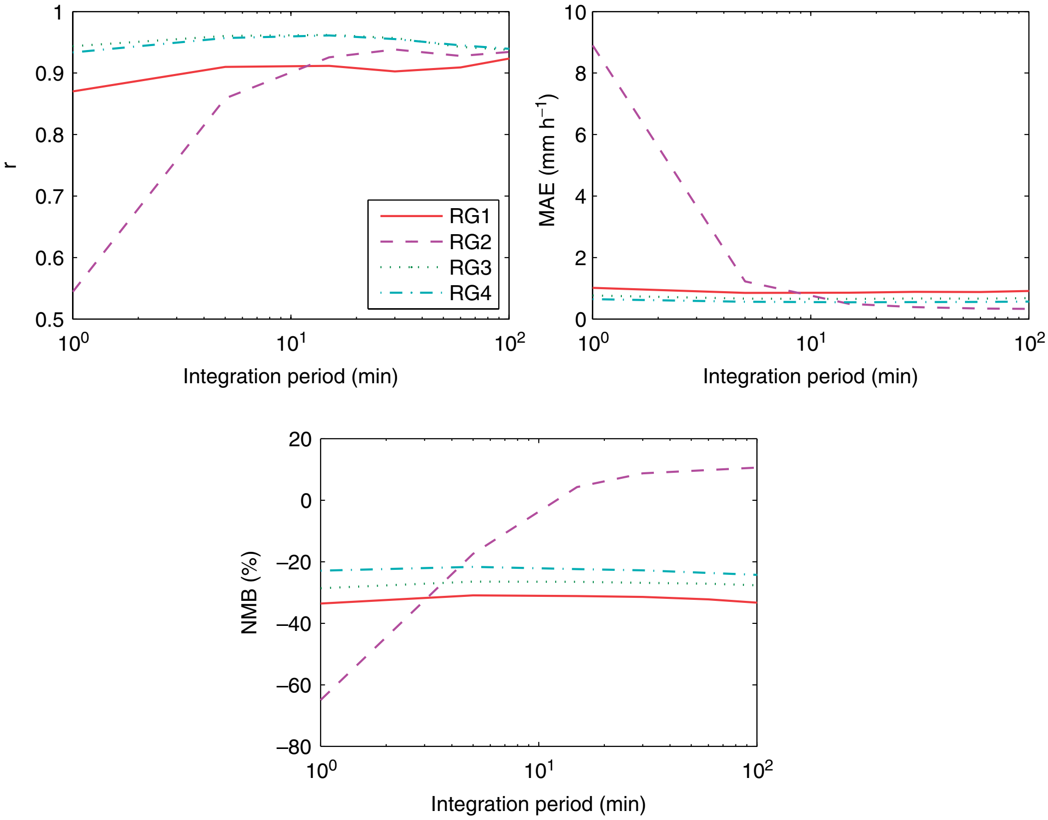

Figure 5. Illustration of changes in Pearson coefficient of correlation *r*, mean absolute error *MAE* (mm h^{-1}), and normalized mean bias *NMB* (%) calculated for the disdrometer with respect to integration period using the four rain gauges as reference.

the disdrometer rain rate R_m at the instant t_i satisfies that time series values from $t_i - 5$ minutes to $t_i + 5$ minutes stay below 10 mm h^{-1} with standard deviation of lesser than 1.5 mm h^{-1}, the corresponding sample is considered as 'stratiform'. In contrary, the sample is considered as 'convective' if R_m values are greater than 10 mm h^{-1}. Figure 8 provides the box-plot distributions of rain rates for the RD, RG1, RG3, and RG4 in stratiform and convective rain clusters. Note that the box-plot distributions for the TBR (RG2) are not shown as TBR is an accumulative device; thus the use of 1 min temporal resolution for stratiform and convective raindrop spectra cannot be possible. The box-plot can be emphasised as a useful way to display the difference of rain rate distributions among the disdrometer and the rain gauges, but without any underlying statistical distribution assumptions. Generally speaking, six statistical measures are depicted by the box-plot, namely, 25th and 75th percentiles of the samples, sample median, upper and lower whiskers, and outliers. From the figure, it can be stated that, the observations are concentrated on the low end of the scale; therefore, the distribution is skewed right. For stratiform rain, the disdrometer sample medians as well as the interquartile ranges are almost similar to those with the rain gauges, agreeing within 1 mm h^{-1} difference. Besides, the whisker lengths and the outliers for the gauge rain rates are relatively more spread out than that of the disdrometer rain rates. On the other hand, for convective rain, the disdrometer median rain rate is noted as 15 mm h^{-1}, differing up to 3 mm h^{-1} when compared to the rain gauges. The differences between the 25th and 75th percentiles of the samples are also in the range of 3–4 mm h^{-1}. Similar to the stratiform case, the range of the rain gauge values are more spread out as compared to the disdrometer values.

4. Conclusions

This short article has presented a Joss–Waldvogel disdrometer derived rainfall estimation appraisal with rain gauges, using an extensive raindrop spectra observation in the period of 2003–2010. Four rain gauges (one tipping bucket and three rapid response drop counting devices) are employed for the assessment. As far as the authors are aware, such long-term study of a JW disdrometer rainfall estimates has never been stated in the literature. The assessments are performed through hourly and yearly rain accumulations between the disdrometer and the four rain gauges. In addition, the results related to rain rate assessment in

Table III. Binning of the eight rain classes and their range in rain rates (mm h^{-1}).

Class	1	2	3	4	5	6	7	8
Rain rate range	0.1–1	1–5	5–10	10–20	20–30	30–50	50–80	>80

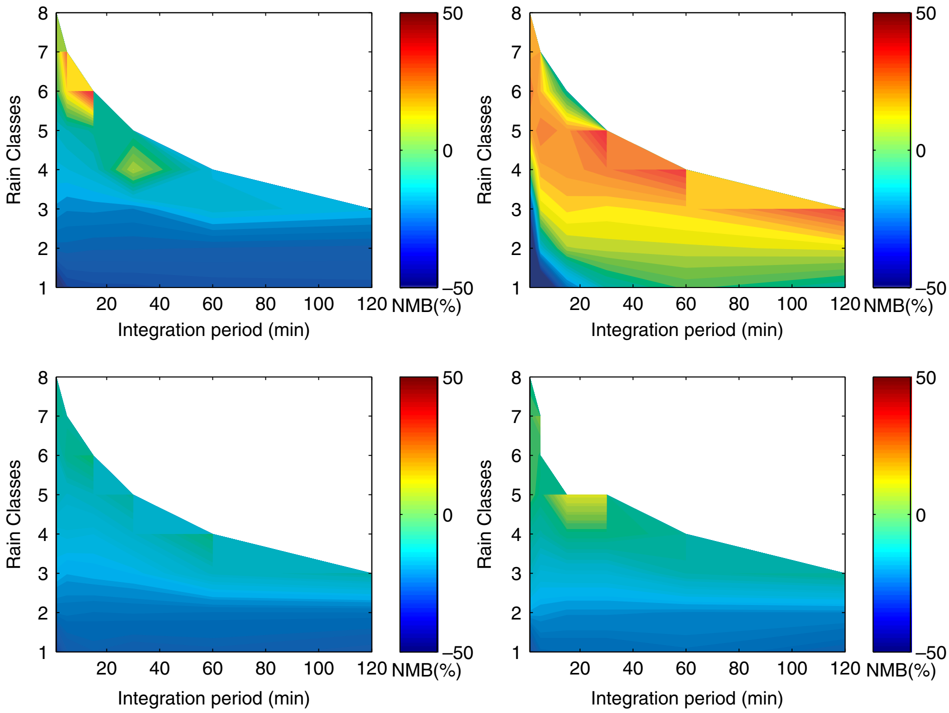

Figure 6. The normalized mean bias of the disdrometer rain rates estimates as a function of rain classes and integration period with respect to the four rain gauges, RG1 (top left), RG2 (top right), RG3 (bottom left), RG4 (bottom right). The binning of the rain classes are given in Table III.

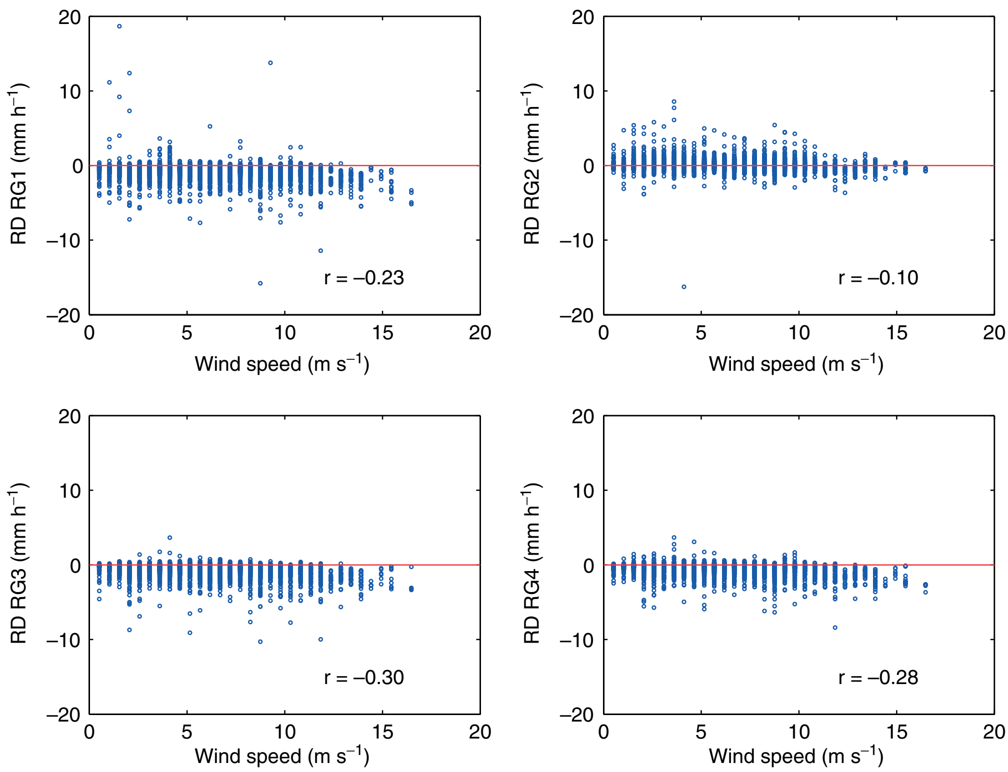

Figure 7. Rain rate difference between the disdrometer and the four rain gauges as a function of wind speed.

view of several associated integrals (e.g. different integration periods and rain classes, influence of wind speeds, and in stratiform and convective rain) are compiled.

It is to be considered that as with any other measurement device, disdrometer and rain gauge both are subject to different sources of uncertainties. A large number of articles regarding rain gauge based rainfall estimation ambiguity have been published in the literature (Habib *et al.*, 2001; Wolff *et al.*, 2005). The notable problems are associated with gauge calibration, sampling and systematic errors along with

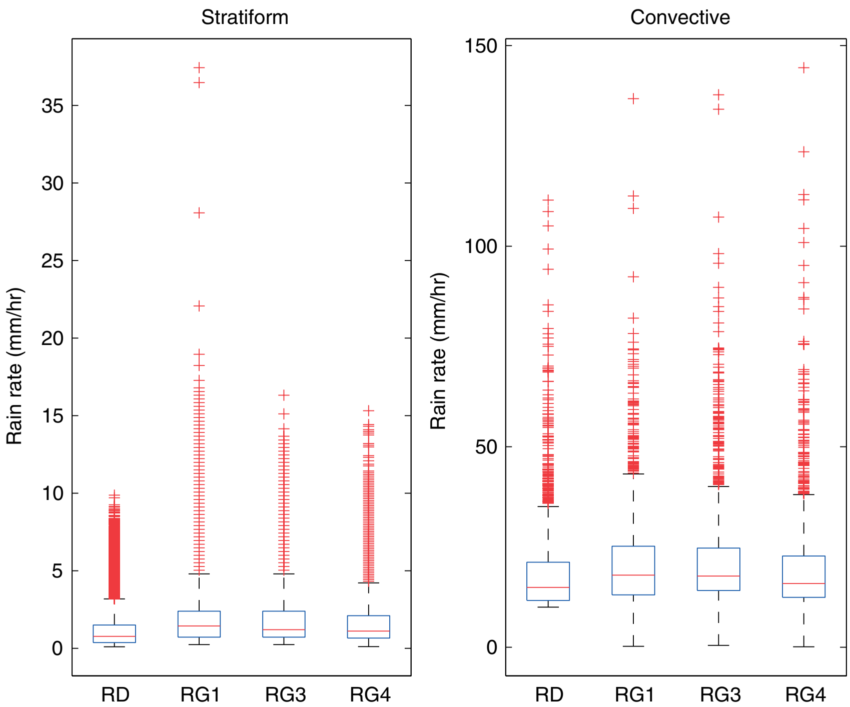

Figure 8. Box plot illustrating the rain rate distributions from the disdrometer (RD), and the three rapid response rain gauges (RG1, RG3, RG4) in stratiform and convective rain clusters.

mechanical problems. Estimating rainfall from the JW disdrometer could also be erratic due to a number of factors, the assumption of fall velocity for example (Vulpiani *et al*., 2009). While comparing between rain gauge and disdrometer, natural and temporal variation of rainfall measurement by two instruments should also to be accounted. Eventually, the rain is a highly variable phenomenon in space and time, and the results presented herein provide an idea of performance agreement between the JW disdrometer and rain gauges, that will be beneficial in many meteorological and hydrological fields.

Acknowledgements

The authors acknowledge the British Atmospheric Data Centre and the Radio Communications Research Unit at the STFC Rutherford Appleton Laboratory for providing the dataset. The authors extend their appreciation to Judith Agnew (RAL Space, STFC) for her support regarding the instrumentation. Thanks to the anonymous reviewers for their insightful comments in improving the manuscript.

References

Atlas D, Ulbrich CW. 1977. Path-integrated and area-integrated rainfall measurement by microwave attenuation in 1–3 cm band. *Journal of Applied Meteorology* **16**: 1322–1331.

Atlas D, Ulbrich CW, Marks FD, Amitai E, Williams CR. 1999. Systematic variation of drop size and radar-rainfall relations. *Journal of Geophysical Research-Atmospheres* **104**: 6155–6169.

Brandes EA, Zhang GF, Vivekanandan J. 2002. Experiments in rainfall estimation with a polarimetric radar in a subtropical environment. *Journal of Applied Meteorology* **41**: 674–685.

Bringi VN, Chandrasekar V, Hubbert J, Gorgucci E, Randeu WL, Schoenhuber M. 2003. Raindrop size distribution in different climatic regimes from disdrometer and dual-polarized radar analysis. *Journal of the Atmospheric Sciences* **60**: 354–365.

Bringi VN, Thurai M, Nakagawa K, Huang GJ, Kobayashi T, Adachi A, Hanado H, Sekizawa S. 2006. Rainfall estimation from C-band polarimetric radar in Okinawa, Japan: comparisons with 2D-video disdrometer and 400 MHz wind profiler. *Journal of the Meteorological Society of Japan* **84**: 705–724.

Bringi VN, Rico-Ramirez MA, Thurai M. 2011. Rainfall estimation with an operational polarimetric c-band radar in the United Kingdom: comparison with a gauge network and error analysis. *Journal of Hydrometeorology* **12**: 935–954.

Campos E, Zawadzki I. 2000. Instrumental uncertainties in Z-R relations. *Journal of Applied Meteorology* **39**: 1088–1102.

Cerro C, Codina B, Bech J, Lorente J. 1997. Modeling raindrop size distribution and Z(R) relations in the Western Mediterranean area. *Journal of Applied Meteorology* **36**: 1470–1479.

Ciach GJ. 2003. Local random errors in tipping-bucket rain gauge measurements. *Journal of Atmospheric and Oceanic Technology* **20**: 752–799.

Distromet L. 1997. *Disdrometer RD-69*, Instruction manual.

Frasson RPD, da Cunha LK, Krajewski WF. 2011. Assessment of the Thies optical disdrometer performance. *Atmospheric Research* **101**: 237–255.

Habib E, Krajewski WF, Kruger A. 2001. Sampling errors of tipping-bucket rain gauge measurements. *Journal of Hydrologic Engineering* **6**: 159–166.

Hagen M, Yuter SE. 2003. Relations between radar reflectivity, liquid-water content, and rainfall rate during the MAP SOP. *Quarterly Journal of the Royal Meteorological Society* **129**: 477–493.

Houze RA, Brodzik S, Schumacher C, Yuter SE, Williams CR. 2004. Uncertainties in oceanic radar rain maps at Kwajalein and implications for satellite validation. *Journal of Applied Meteorology* **43**: 1114–1132.

Jaffrain J, Berne A. 2011. Experimental Quantification of the sampling uncertainty associated with measurements from PARSIVEL disdrometers. *Journal of Hydrometeorology* **12**: 352–370.

Joss J, Waldvogel A. 1967. A spectrograph for raindrops with automatic interpretation. *Pure and Applied Geophysics* **68**: 240.

Joss J, Waldvogel A. 1977. Some observations on joss-waldvogel rainfall disdrometer – reply. *Journal of Applied Meteorology* **16**: 112–113.

Kozu T, Iguchi T, Kubota T, Yoshida N, Seto S, Kwiatkowski J, Takayabu YN. 2009. Feasibility of raindrop size distribution parameter estimation with TRMM precipitation radar. *Journal of the Meteorological Society of Japan* **87**: 53–66.

Lee G. 2006. Sources of errors in rainfall measurements by polarimetric radar: variability of drop size distributions, observational noise, and variation of relationships between R and polarimetric parameters. *Journal of Atmospheric and Oceanic Technology* **23**: 1005–1128.

Lee G, Zawadzki L. 2006. Radar calibration by gage, disdrometer, and polarimetry: Theoretical limit caused by the variability of drop size distribution and application to fast scanning operational radar data. *Journal of Hydrology* **328**: 83–97.

Marzano FS, Cimini D, Montopoli M. 2010. Investigating precipitation microphysics using ground-based microwave remote sensors and disdrometer data. *Atmospheric Research* **97**: 583–600.

Matrosov SY, Clark KA, Martner BE, Tokay A. 2002. X-band polarimetric radar measurements of rainfall. *Journal of Applied Meteorology* **41**: 941–952.

Miriovsky BJ, Bradley AA, Eichinger WE, Krajewski WF, Kruger A, Nelson BR, Creutin JD, Lapetite JM, Lee GW, Zawadzki I, Ogden FL. 2004. An experimental study of small-scale variability of radar reflectivity using disdrometer observations. *Journal of Applied Meteorology* **43**: 106–118.

Montopoli M, Marzano FS, Vulpiani G. 2008. Analysis and synthesis of raindrop size distribution time series from disdrometer data. *IEEE Transactions on Geoscience and Remote Sensing* **46**: 466–478.

Moumouni S, Gosset M, Houngninou E. 2008. Main features of rain drop size distributions observed in Benin, West Africa, with optical disdrometers. *Geophysical Research Letters* **35**: L23807, DOI: 10.1029/2008GL035755.

Norbury JR, White WJ. 1971. Rapid-response rain gauge. *Journal of Physics E-Scientific Instruments* **4**: 601.

Park SG, Maki M, Iwanami K, Bringi VN, Chandrasekar V. 2005. Correction of radar reflectivity and differential reflectivity for rain attenuation at X band. Part II: evaluation and application. *Journal of Atmospheric and Oceanic Technology* **22**: 1633–1655.

Radhakrishna B, Rao TN. 2010. Differences in cyclonic raindrop size distribution from southwest to northeast monsoon season and from that of noncyclonic rain. *Journal of Geophysical Research-Atmospheres* **115**: D16205, DOI: 10.1029/2009JD013355.

Rico-Ramirez MA, Cluckie ID, Shepherd G, Pallot A. 2007. A high-resolution radar experiment on the island of Jersey. *Meteorological Applications* **14**: 117–129.

Ryzhkov AV, Zrnic DS. 1995. Comparison of dual-polarization radar estimators of rain. *Journal of Atmospheric and Oceanic Technology* **12**: 249–256.

Sheppard BE. 1990. Effect of irregularities in the diameter classification of raindrops by the joss-waldvogel disdrometer. *Journal of Atmospheric and Oceanic Technology* **7**: 180–183.

Sheppard BE, Joe PI. 1994. Comparison of raindrop size distribution measurements by a joss waldvogel disdrometer, a pms 2dg spectrometer, and a poss doppler radar. *Journal of Atmospheric and Oceanic Technology* **11**: 874–887.

Sieck LC, Burges SJ, Steiner M. 2007. Challenges in obtaining reliable measurements of point rainfall. *Water Resources Research* **43**: W01420, DOI: 10.1029/2005WR004519.

Tokay A, Kruger A, Krajewski WF, Kucera PA, Pereira AJ. 2002. Measurements of drop size distribution in the southwestern Amazon basin. *Journal of Geophysical Research-Atmospheres* **107**: NO. D20, 8052, DOI: 10.1029/2001JD000355.

Tokay A, Wolff DB, Wolff KR, Bashor P. 2003. Rain gauge and disdrometer measurements during the keys area microphysics project (KAMP). *Journal of Atmospheric and Oceanic Technology* **20**: 1460–1477.

Tokay A, Bashor PG, Wolff KR. 2005. Error characteristics of rainfall measurements by collocated Joss-Waldvogel disdrometers. *Journal of Atmospheric and Oceanic Technology* **22**: 513–527.

Vulpiani G, Giangrande S, Marzano FS. 2009. Rainfall estimation from polarimetric s-band radar measurements: validation of a neural network approach. *Journal of Applied Meteorology and Climatology* **48**: 2022–2036.

Wang JX, Fisher BL, Wolff DB. 2008. Estimating rain rates from tipping-bucket rain gauge measurements. *Journal of Atmospheric and Oceanic Technology* **25**: 43–56.

Wolff DB, Marks DA, Amitai E, Silberstein DS, Fisher BL, Tokay A, Wang J, Pippitt JL. 2005. Ground validation for the tropical rainfall measuring mission (TRMM). *Journal of Atmospheric and Oceanic Technology* **22**: 365–380.

Yuter SE, Kingsmill DE, Nance LB, Loffler-Mang M. 2006. Observations of precipitation size and fall speed characteristics within coexisting rain and wet snow. *Journal of Applied Meteorology and Climatology* **45**: 1450–1464.

